Am J Transl Res 2018;10(1):246-255
www.ajtr.org /ISSN:1943-8141/AJTR0069653

Original Article

Negatively-charged aerosol improves burn wound healing by promoting eNOS-dependent angiogenesis

Jingling Zhao, Fei Zhou, Lei Chen, Bin Shu, Qiyi Zhai, Jun Wu, Xusheng Liu, Shaohai Qi, Yingbin Xu

Department of Burns, The First Affiliated Hospital of Sun Yat-sen University, Guangzhou, China

Received November 23, 2017; Accepted December 23, 2017; Epub January 15, 2018; Published January 30, 2018

Abstract: Aerosols exist in the form of liquid or solid particles that stably suspending in air. Our previous studies have found that aerosol can accelerate chronic wound healing. However, the biological effects of aerosol in burn wound healing and the underlying molecular mechanism remain unclear. This study aimed to investigate the effects of aerosol on the healing of deep partial-thickness burn wounds and its regulatory mechanisms. By employing a self-controlled model of rats, we demonstrated that aerosol treatment not only increased the healing rate, but also improved the healing quality of deep partial-thickness burn wounds. Besides, the excessive inflammatory responses in the burn wounds were inhibited, and the angiogenesis was increased after aerosol treatment. It did so by upregulating the expression of eNOS/NO, as well as the VGEF expression during the wound healing process. Our results demonstrate that the function of aerosol in promoting burn wound healing is achieved by activating eNOS/NO pathway.

Keywords: Aerosol, wound healing, angiogenesis

Introduction

A series of physiopathological changes in the body after burn injury is mainly caused by the burn wounds [1]. The treatment of burn wounds directly affects the prognosis of patients [2]. Therefore, exploring effective ways to promote wound healing is crucial for burns management.

Aerosol is a system of tiny liquid or solid particles with the size of 0.01 μm-100 μm in diameter [3]. It will be defined as negatively-charged aerosol when the aerosol carrying a certain amount of negative charge. It has a long history to apply the negatively-charged aerosols in the field of biomedical science [4]. Since the negatively-charged aerosol has the antibacterial effects, it has been used as an effective sterilizing method in the 1950s [5, 6]. In recent years, inhalation of aerosol was widely used in treating the respiratory diseases, such as asthma and bronchitis, playing important roles in anti-inflammation and spasmolysis [7, 8]. More interestingly, a clinical trial that conducted by our research team have found that negatively-charged aerosol acted as a effective bactericidal factor, and accelerated chronic wound healing by controlling hospital infection acquirement [9]. Besides, another experiment also showed that the negatively-charged aerosol has potential therapeutic effects in treating the acute wounds, such as burn wounds. However, despite its proven therapeutic effects, little is known about the molecular mechanisms underlying the action of negatively-charged aerosol in burn wounds.

Nitric oxide (NO), a highly reactive free radical that serves as a messenger molecule in various physiological and pathological processes [10], is formed by the oxidation of Larginine through the activation of three different NO synthase (NOS) isoforms, including neuronal NOS (nNOS), inducible NOS (iNOS), and endothelial NOS (eNOS) [11, 12]. Studies have shown that eNOS/NO functioned as powerful angiogenic mediators and can induce endothelial cell proliferation, migration, and tube formation [13, 14]. The angiogenesis and wound healing were delayed in the eNOS deficient mice [15], whereas upregulation of eNOS expression and NO production significantly promoted wound healing [16].

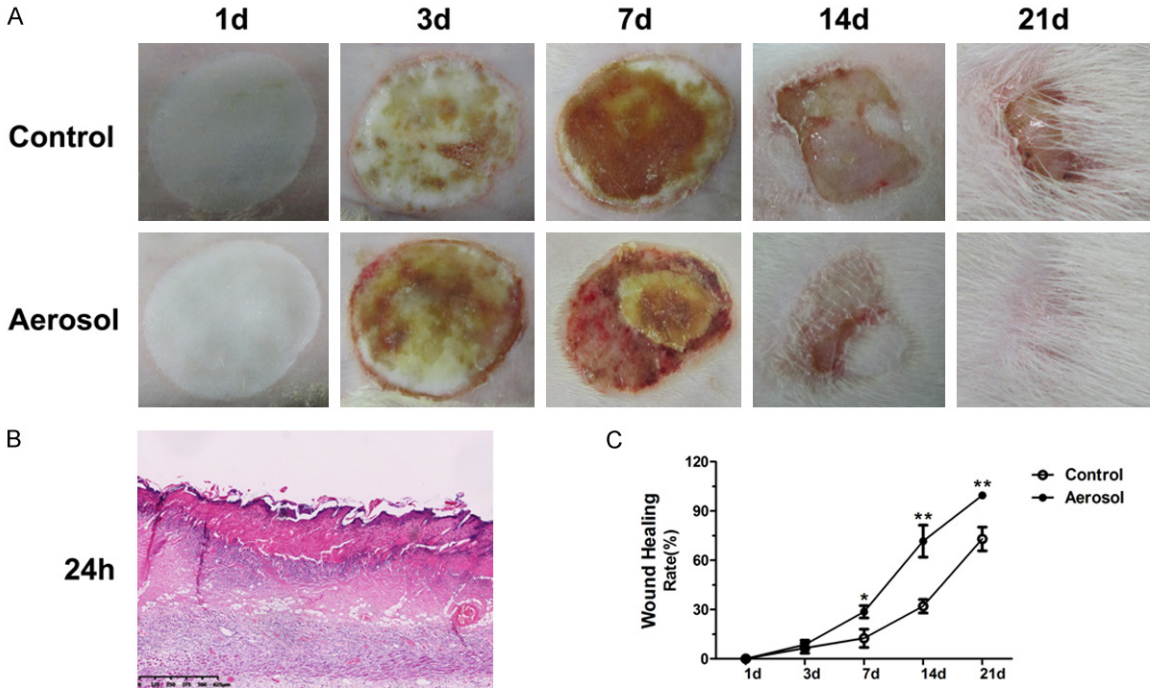

Figure 1. The speed of burn wound healing in the two groups. A. Photographs showing the macroscopic wound healing in both the control and aerosol treatment groups at different time points following the burn event. B. The confirmation of the depth of deep partial-thickness burn wounds in rats by H&E staining. C. Graph showing the quantification of wound healing rate in the two groups. The healing rate of the aerosol-treated wounds was significantly faster than the wounds without any treatments on the 7th, 14th, and 21st post-burn days (n=6) ($^{*}P<0.05$, $^{**}P<0.01$).

In this study, we investigated the effect of negatively-charged aerosol in burn wound healing, and found that the negatively-charged aerosol can accelerate the burn wounds healing by promoting the angiogenesis process, and the activation of eNOS/NO pathway served as the potential mechanism.

Materials and methods

Animal experiment

A total of thirty-four sex-matched Sprague-Dawley rats (180-220 g) that purchased from the Experimental Animal Research Laboratory at Sun Yat-sen University in China were individually caged under specific pathogen-free (SPF) conditions. The feed and treatment of the rats were carried out strictly according to the Committee on Publication Ethics (COPE) guidelines.

The deep partial-thickness burn wounds in rates were created using a 2.5-cm-diameter electrically heated brass rod as described in our previous study [17]. Briefly, the animals were injected intraperitoneally with 3 ml/kg chloral hydrate (10%) for anaesthesia. The hair on the backs of the rats was removed by an electric shaver. Deep partial-thickness burn wounds that were 0.5-1 cm off the midspinal line were made on each side of the dorsum of the rats by application of the electrically heated brass rod for 8 s with a constant pressure and temperature (1 kg, 80°C). The depth of burn wounds were confirmed 24 h later by H&E staining (**Figure 1B**). Paired wounds on the same rat were randomly divided into the experimental group and the control group. The experimental group was treated with a negative-charged aerosols therapeutic apparatus (NB-I, Siqi Electronic Equipment Co., China). Aerosols with the size of 5 μm diameter were generated by this apparatus. The operative distance of the apparatus is 30 cm apart from the wounds, and the treatment lasted for 1.5 h each time. The wounds without any treatments were used as controls, and all the wounds were covered with sterile gauze and bandaged. The aerosol treatment was applied twice a day, and the skin biopsies were harvested on the 1st, 3rd, 7th, 14th, and 21st days, respectively.

Table 1. The primer sequence of the inflammatory genes that were detected

Primer	Forward (5'-3')	Reverse (5'-3')
IL-1β	CAGCCTCAGCGAAGAGACCTT	ACTGTGGTGTGCTCAGAATCC
TNF-α	CCAGGTTCTCTTCAAGGGACAA	CTCCTGGTATGAAATGGCAAATC
IL-8	GGCTTGCCTTGACCCTGAA	ATCGGTGCAATCTATCTTCTTTCTC
IL-6	CCAAGACCATCCAACTCATCTTG	CACAGTGAGGAATGTCCACAAAC
β-actin	CCAGGTTCTCTTCAAGGGACAA	CTCCTGGTATGAAATGGCAAATC

Wound analysis

The burn wounds were digitally photographed at the indicated time intervals, and the wound closure was assessed using Image J software (National Institutes of Health, Bethesda, MD, USA). The wound areas were standardized by comparison with the original wound size, and the healing rate was expressed as a percentage of wound closure: [(day 0 area-day n area)/(day 0 area)] ×100% (n=1, 3, 7, 14 or 21).

Histology and immunohistology

Harvest tissues were fixed with paraformaldehyde (4%, PFA) overnight followed by dehydration and embedded in paraffin. Serial 5-μm sections were cut and stained with haematoxylin and eosin (HE) and Masson's trichrome.

For immunohistochemical staining, the activity of endogenous peroxidase was quenched by incubation with 1% hydrogen peroxide for 15 min followed by treatment of antigen retrieval solution (Dako, Carpinteria, CA). The sections were then incubated with primary antibodies against rat CD31 (1:1000 dilution, BD Biosciences, San Jose, CA) and eNOS (1:1000 dilution, Abcam, Cambridge, MA) at 4°C overnight. After thorough washing, the sections were incubated with biotinylated secondary antibody (Vector laboratories, Burlingame, CA) for 1 h, followed by incubation with avidin-biotin complex (Elite ABC kit; Vector Laboratories) for 1 h. Color was developed in 3,3'-diaminobenzidine (DAB) and nuclei were stained with hematoxylin (Sigma-Aldrich, St. Louis, MO). Negative control staining experiments were performed by omission of the primary antibody. Images were captured using a light microscope (BX51 WI Olympus, Allen, PA).

For immunofluorescent staining, a double-labeling technique was applied to analyze the proliferation of endothelial cells using anti-CD31 (1:200 dilution, BD Biosciences,) and anti-Ki67 (1:400 dilution, Abcam) antibodies. Briefly, the sections were blocked with 5% BSA for 2 h and incubated with primary antibodies at 4°C overnight. After washing, the sections were further incubated with secondary antibodies (Vector laboratories) for 1 h in the dark. Subsequently, the sections were incubated in 4'6-diamidino-2 phenylindole (DAPI) for nuclear staining. Images were obtained with a fluorescence microscope (Carl Zeiss) and were merged using Image-Pro Plus v. 6.0 software.

Microvessel density (MVD) and proliferating capillary index (PCI) quantification

The MVD has been widely used to assess blood vessel number. Here, an endotheliocyte cluster of pale brown colour of CD31 expression was identified as a blood vessel, regardless of whether the lumen or red blood cells were present [18]. For the PCI, which was used to determine the proliferation of endothelial cells, was quantified by calculating the ratio of the number of microvessels with proliferating endothelial cells (Ki67) to the total number of microvessels (CD31) [19]. The vessels were counted under a power field of 10×20 in 5 randomly selected fields from 3 separate sections of each sample. The MVD and PCI was quantified as the average number of microvessels per viewing field.

Quantitative real-time PCR assay

Total RNA was isolated using TRIzol Reagent (Invitrogen, Carlsbad, CA, USA), and was reverse-transcribed into cDNA using a thermocycler (S1000, Bio-Rad, Berkeley, CA, USA) and the First Strand cDNA Synthesis Kit (Fermentas), according to the manufacturer's protocol. Real-time RT-PCR was performed using the SYBR qPCR mix (Invitrogen), and the thermocycling profile was as follows: an initial denaturation step at 95°C (1 min), followed by 40 cycles of denaturation at 95°C (15 s), annealing at 60°C (15 s) and extension at 72°C (60 s). Each sample was run in triplicate, and the relative gene expression was quantified using the $2^{-\Delta\Delta Ct}$ method [20]. The primer sequences that used in this study were collected in **Table 1**.

Transmission electron microscopy

The skin sections were fixed in glutaraldehyde (2.5%) for 24 h and osmium tetroxide (1.0%) for 1.5 h, respectively. Then the sections were dehydrated in a graded ethanol series, followed by embedded in Epon812. Ultrathin sections were cut using an ultramicrotome device and were mounted on slit grids that coated with formavar. Ultrathin sections were stained with uranyl acetate and lead citrate, and then was observed under a transmission electron microscope (Hitachi H-500).

Measurements of nitrite and nitrate NO

The in vivo microdialysis was carried out firstly [21]. Briefly, the rats were anesthetized and maintained at 37°C. Microdialysis probes (CMA Microdialysis AB, Kista, Sweden) that treated with Heparin sodium (100 U/mL) were connected though polyethylene, which was tubed to a microsyringe at one end, and punctured into the skin dermis layer close to the wound edges at the other end. Phosphate buffer (10 mM, pH 7.4) was perfused for 1 h at a constant flow rate of 2.0 μL/min, and the perfusates were collected via polyethylene tubing.

The quantification of NO production in the skin wounds was performed by simultaneously measuring the NO metabolites of nitrite ($NO2^-$) and nitrate ($NO3^-$) in the microdialysate [22]. Briefly, 10 μL of the microdialysate fraction was injected into an NO-detector (Eicom, San Diego, CA). The $NO2^-$ and $NO3^-$ in the microdialysate were separated by a reverse-phase separation column (Eicom, San Diego, CA). The absorbance of the product was detected at 540 nm using a flow-through spectrophotometer (NOD-10, Eicom, San Diego, CA). The concentrations of $NO2^-$ and $NO3^-$ were obtained using a standard curve.

Statistical analyses

The results were expressed as means ± standard deviation. Comparisons of the healing rate, microvascular density, proliferating capillary index and inflammatory cytokines expression between control and aerosol groups at the same time point were conducted using Student's t test. The differences between two groups at different time points were compared using one-way ANOVA, followed by the Bonferroni test. All statistical analyses were performed by SPSS 18.0 software (SPSS, Chicago, IL, USA). A p value <0.05 was considered to be statistically significant.

Results

Aerosols accelerated burn wound healing in rats

The deep partial-thickness burn wounds were created on the back of rats, and the depth of wounds was confirmed within 24 h after burns (**Figure 1B**). In the aerosol treatment group, the crusta began to separate from the wound margins on the 3rd day after burning and fell off completely on the 14th day, when the residual wound area was less than 40%. The wounds reached complete closure, and the newborn hair can be clearly observed on the 21st day. In contrast, in the control group, the decrustation of the wounds was delayed, which can be observed until the 7th day, and the epithelization was much slower compared with that in the experimental group. There was more than 30% wound area left in the control group on the 21st day, when the wounds healed completely in the aerosol treatment group (**Figure 1A**). The quantification of wound healing rate was shown in **Figure 1C**, and the healing rate of the aerosol-treated wounds was significantly faster than the wounds without any treatments on the 7th, 14th, and 21st post-burn days.

Aerosols improved the quality of burn wound healing in rats

On the 3rd day after burning, there were edema and a large number of inflammatory cells infiltration in the control group, while only a relatively small amount of inflammatory cells can be detected in the aerosol-treated wounds. The monolayer epithelium has already formed in aerosol-treated wounds on the 7th day, when the epidermal cells were still absence in the control group. In addition, the proliferation of dermal fibroblasts was active in the aerosol-treated wounds, while the nuclear pyknosis can be observed in the control group (**Figure 2B**). In the late stages of wound healing, the epidermal layer was thicker and new blood vessels were abundant in the aerosol-treated wounds. However, the number of new blood vessels was less and the epidermal layer was thinner and disorganized in the control group (**Figure 2A**).

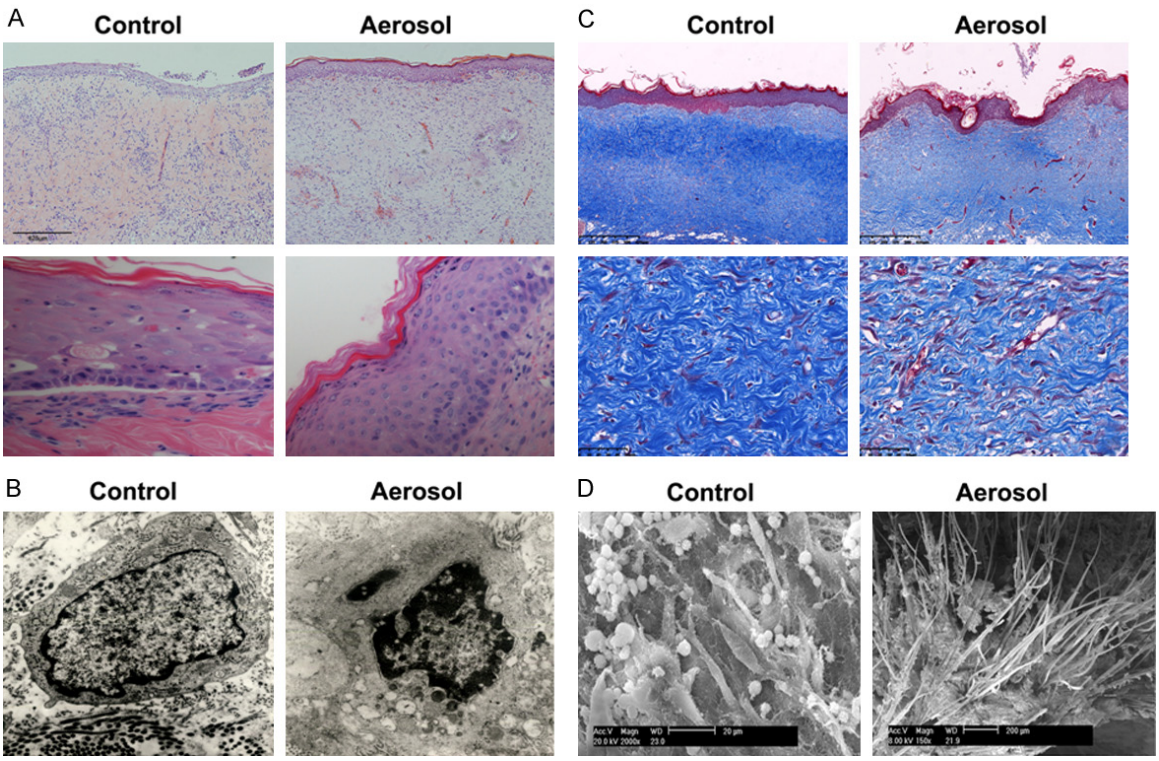

Figure 2. The quality of burn wound healing in the two groups. A. H&E staining showing the histological changes in burn wounds in the two groups at days 21 after the burn event. The epidermal layer was thicker and new blood vessels were abundant in the aerosol-treated wounds. B. Dermal fibroblasts in the two groups were observed and photographed by the transmission electron microscopy. The proliferation of dermal fibroblasts was active in the aerosol-treated wounds, while the nuclear pyknosis can be observed in the control group. C. Masson's trichrome staining showing the organization of dermal collagen fibers in the two groups. The collagen fibrils were distributed compactly and regularly in the aerosol-treated wounds, which were disorganized in the control group. D. The regenerative accessory structures in the burn wounds were observed by the transmission electron microscopy. The accessory structures, such as hair follicles were obviously regenerated in the aerosol-treated wounds.

Masson's trichrome staining was used to show the dermal collagen fibers. As shown in **Figure 2C**, the collagen fibrils were distributed compactly and regularly in the aerosol-treated wounds, which were disorganized in the control group. The accessory structures, such as hair follicles were obviously regenerated in the aerosol-treated wounds, while these structures were destroyed or missing in the control group (**Figure 2D**).

Aerosols promoted the angiogenesis in the burn wounds

Angiogenesis is an important event in the process of wound healing, which is seriously blunted in burn wound. Here, we evaluated the angiogenesis by immunostaining endothelial cell marker CD31. As shown in **Figure 3A**, **3B**, there were a small number of CD31-positive cells in both groups on the 1st and 3rd days. The number of endothelial cells was obviously increased beginning on the 7th day, peaked on the 14th day, and then decreased slightly on the 21st day. To quantify the number of microvessels, the MVD was used and result showed that aerosol-treated wounds had much higher MVD than the control group from the 7th to the 21st days.

In addition, we used a combination of the specific markers CD31 and Ki67 to simultaneously immunostain endothelial cells and proliferating cells to quantitatively assess the proliferation status of the endothelial cells in the wounds (**Figure 3C**). PCI is quantified by the percentage of microvessels with Ki67-positive endothelial cell nuclei, and results showed that the PCI values increased from the 1st to the 3rd day, and the aerosol-treated wounds had higher PCI val-

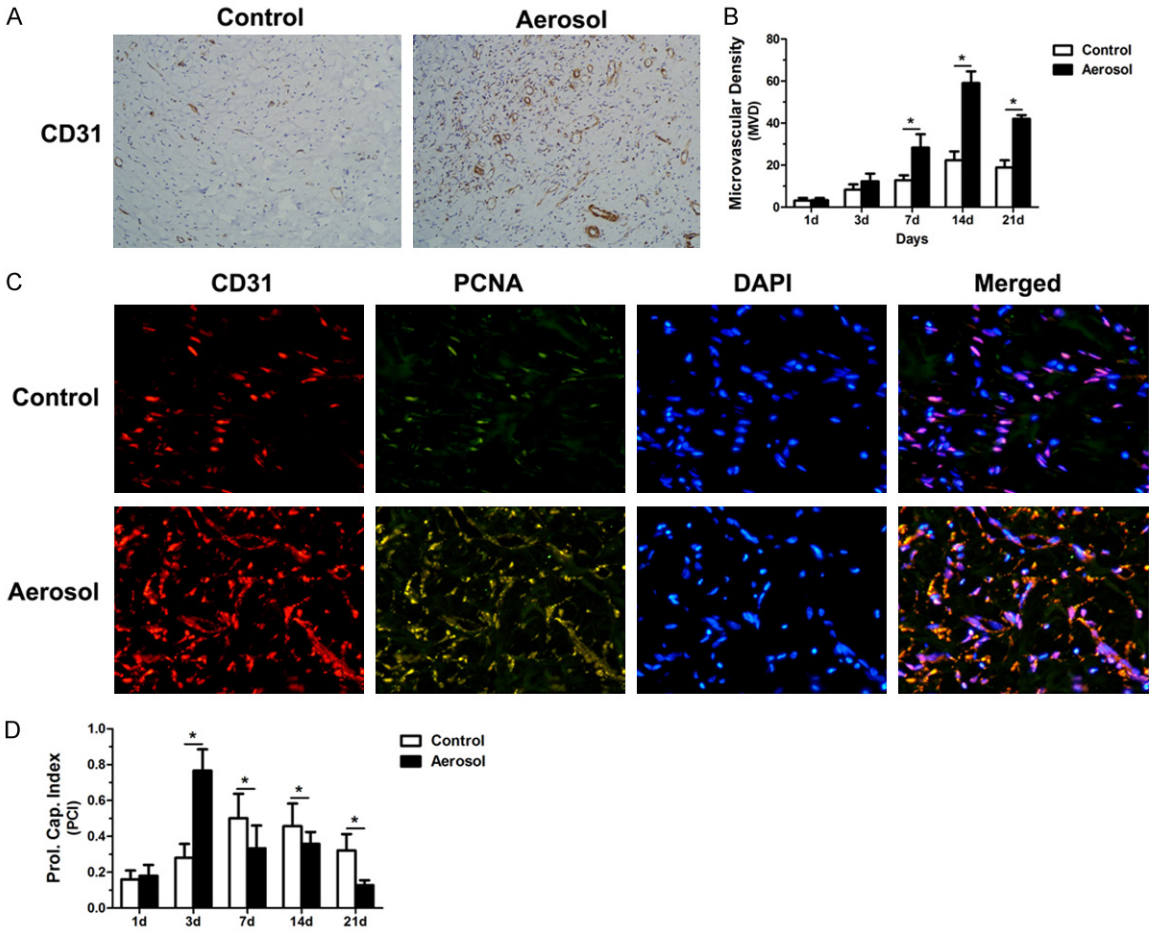

Figure 3. The angiogenesis process in the burn wounds during the wound healing. A. Immunohistochemical staining showing the CD31-positive microvessels in burn wounds. Representative images at days 14 after the burn event are shown. B. Quantification of the microvessel density (MVD) in the two groups at different time intervals. The aerosol-treated wounds had much higher MVD than the control group from the 7th to the 21st days. C. Representative examples of double staining of PCNA/CD31 (green, PCNA; red, CD31; nucleus, blue) in skin sections from the control group and the aerosol t treatment group at day 7 after the burn event. D. Quantitative comparison of the proliferating capillary index (PCI) in the two groups. The PCI was used to assess the percentage of microvessels with proliferating endothelial cells (n=6). The PCI increased from the 1st to the 3rd day, and the aerosol-treated wounds had higher PCI values than the control group on the 3rd day. The PCI decreased gradually from the 7th to the 21st day in the aerosol-treated wounds, and they were much lower than that in the control group (n=6) ($^{*}P<0.05$, $^{**}P<0.01$).

ues than the control group on the 3rd day. The PCI values decreased gradually from the 7th to the 21st day in the aerosol-treated wounds, and they were much lower than that in the control group (**Figure 3D**).

Aerosols inhibited the inflammatory cytokines expression in the burn wounds

Studied have demonstrated that the inflammatory cytokines, such as IL-1β, TNF-α, IL-8 and IL-6 are over-expressed in the burn wounds, and the expression levels of these cytokines are involved in the healing rate and quality of burn wounds [23]. Here we detected the expression of these cytokines in the burn wounds of rats that treated with or without aerosol. By PCR assay, we found that the expression of IL-1β, TNF-α, IL-8 and IL-6 in the wounds peaked on the 3rd day, and the expression levels in the aerosol-treated group were much lower than that in the control group. The expression of IL-1β, TNF-α, IL-8 and IL-6 decreased gradually in both groups from the 7th to the 21st days, and these inflammatory cytokines expression were significantly reduced after aerosol treatment when compared with the control group (**Figure 4A-D**), suggesting that aerosol treat-

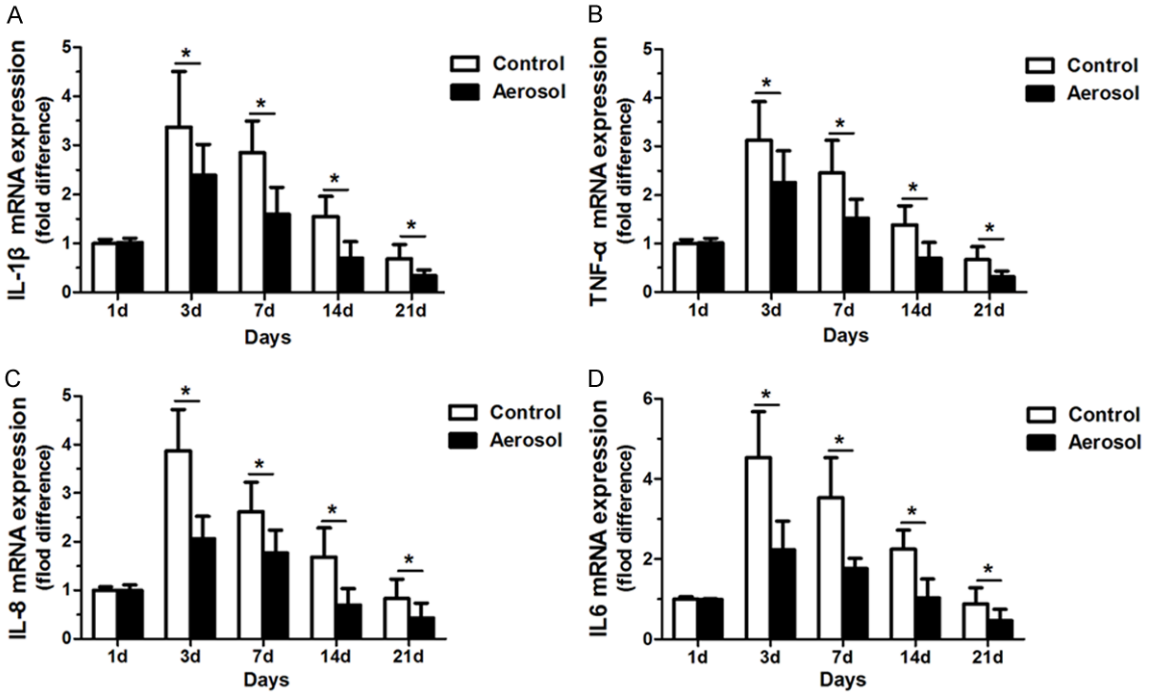

Figure 4. The mRNA expression of pro-inflammatory cytokines in the burn wounds during the wound healing. A. The expression of IL-1β in the two groups at different time intervals. B. The expression of TNF-α in the burn wounds of two groups. C. The expression of IL-8 in the two groups. D. The expression of IL-6 in the two groups at different time intervals. The expression of IL-1β, TNF-α, IL-8 and IL-6 in the wounds peaked on the 3rd day, and the expression levels in the aerosol-treated group were much lower than that in the control group. The expression of IL-1β, TNF-α, IL-8 and IL-6 decreased in both groups from the 7th to the 21st days, and these expression were significantly reduced after aerosol treatment when compared with the control group (n=6) (*P<0.05).

ment can inhibit the excessive inflammatory responses in the burn wounds.

Aerosols increased the eNOS/NO/VEGF signaling pathways in the burn wounds

Given that the eNOS/NO pathway plays a critical role in the process of angiogenesis, and the downstream of it, such as VEGF functions as one of the most important pro-angiogenic factors [24]. Here we detected the expression of eNOS/NO/VEGF during the burn wound healing. **Figure 5A** shows the immunohistochemistry analysis of eNOS expression in burn wounds of each experimental group on the 14th day after burning. The control group exhibited sporadic staining of eNOS, whereas the aerosol-treated group exhibited strong and extensive pale brown staining of eNOS, which mainly located around the newly formed microvessels. The relative level of positive eNOS staining in the aerosol-treated group was much higher than that in the control group from the 3rd to the 21st days (**Figure 5B**).

The extracellular levels of NO that extracted from the burn wound was shown in the **Figure 5C**. During the healing processes, the expression of NO obviously increased beginning on the 3rd day, peaked on the 14th day, and then decreased slightly on the 21st day. When compared with the control group, which exhibited low levels of NO, the expression of NO was much higher in the aerosol-treated group from the 3rd to the 21st days.

Furthermore, we detected the expression of VEGF, an important pro-angiogenic cytokine during the wound healing. As shown in **Figure 5D**, the expression of VEGF increased slightly on the 3rd day, when the aerosol-treated group exhibited higher level expression than that in the control group. The expression of VEGF continued increasing, peaked on the 14th day and then reduced slightly on the 21st day. When compared with the control group, the expression of VEGF in the aerosol-treated group increased significantly on the above time points.

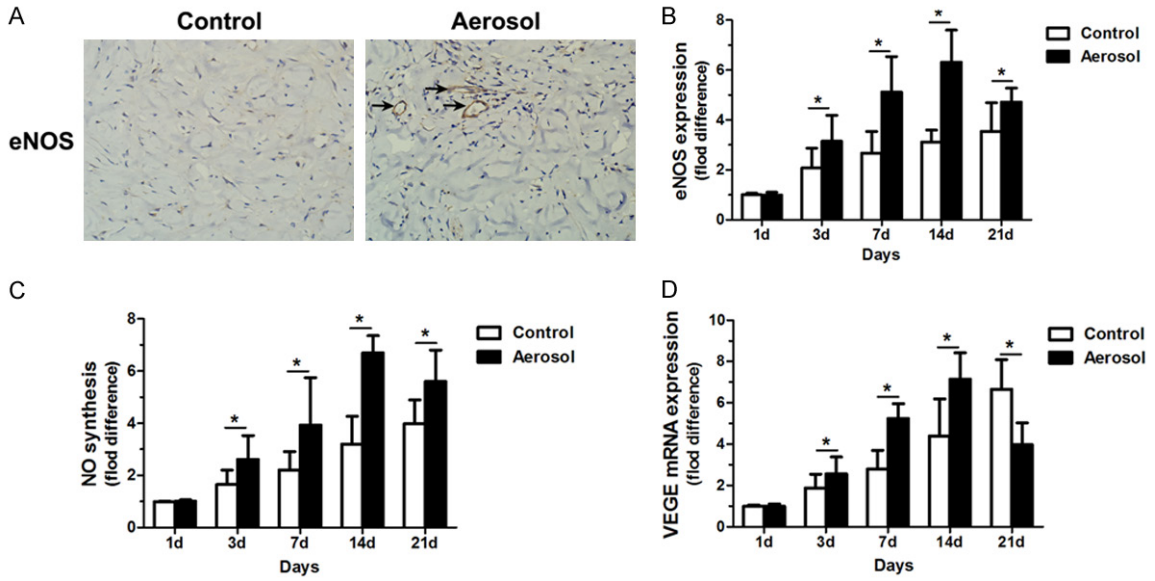

Figure 5. The activation of eNOS/NO/VEGF signaling pathway during the wound healing in the two groups. A. Immunohistochemical staining showing the expression and location of eNOS in burn wounds. Representative images at days 14 after the burn event are shown. The control group exhibited sporadic staining of eNOS, whereas the aerosol-treated group exhibited strong and extensive pale brown staining of eNOS, which mainly located around the newly formed microvessels. B. Quantification of the expression of eNOS in the two groups at different time intervals. The relative level of positive eNOS staining in the aerosol-treated group was much higher than that in the control group from the 3rd to the 21st days. C. Quantification of the extracellular levels of NO that extracted from the burn wounds in the two groups at different time intervals. The expression of NO was much higher in the aerosol-treated group than that in the control group from the 3rd to the 21st days. D. The mRNA expression of VEGF in the burn wounds of two groups. When compared with the control group, the expression of VEGF in the aerosol-treated group increased significantly from the 3rd to the 21st days (n=6) (*P<0.05).

Discussion

The main objective in burns management is accelerating the rate of wound healing, shorten healing time, restoring the appearance and function of the burned areas as much as possible [2]. In this study, we used the negatively-charged aerosol to treat deep partial-thickness burn wounds in rats, and found that the healing rate significantly increased after negatively-charged aerosol treatment, and the quality of healing, including the thickness of new-formed epidermis, the arrangement of collagen fibers and the renew of skin appendage structures were also improved.

The negatively-charged aerosol carried a certain amount of negative charge, which has been demonstrated as an effective method for promoting wound healing [25]. Studies have shown that the bioelectricity system that stably exists in the human body has repair effects for injured tissues [26]. The bioelectricity system was destroyed, and lost the function of promoting repairing under special conditions, when the exogenous negative air ion application can promote wound repair by simulating the endogenous bioelectricity. The mechanisms underlying it include the activation of immune cells, elevating the expression of growth factors, such as PDGF, and affecting the vitality of superoxide dismutase (SOD) [27].

Aerosol, which is defined as the mixture of liquid or solid particles that stably suspending in the air, has been proved to had therapeutic effects in diseases, such as respiratory diseases [4]. However, the the variety of their shapes, sizes, densities and electrical charge will affect the behavior of aerosol. Our previous researches have shown that the aerosol carrying a certain amount of negative charge can promote the wound healing, especially for the chronic wounds [9]. However, the effects of negatively-charged aerosol on acute wounds healing, such as burn wound, and the potential mechanism underlying it was still unclear.

In this study, we found that the negatively-charged aerosol application remarkably redu-

ced the inflammation in the burn wounds by decreasing the pro-inflammatory cytokines expression. More importantly, the angiogenesis, the critical process of tissue repair was also improved after negatively-charged aerosol treatment, suggesting that promoting angiogenesis is the main mechanism for negatively-charged aerosol in improving burn wound healing.

Among the various factors that regulate the angiogenesis, eNOS/NO functioned as an important motivator [28]. Researches have found that intractable wounds with endothelial dysfunction, such as impaired diabetic wounds showed reduced activation of eNOS and increased reactive oxygen species, which account for the reduced synthesis and bioavailability of NO and increased NO consumption, respectively [29]. However, increasing NO biosynthesis and bioavailability via the direct up-regulation of eNOS expression not only protected the endothelial function and stimulated the angiogenesis, but also promoted the healing rate and quality of wounds [30, 31]. In line with previous studies, in this study we found that the expression of eNOS/NO, and the downstream VEGF in the wounds were obviously increased after the negatively-charged aerosol treatment, demonstrating that the eNOS/NO activation is involved in the aerosol-induced angiogenesis and wound repair.

In summary, the negatively-charged aerosol accelerates burn wounds healing by promoting the angiogenesis process, and the activation of eNOS/NO pathway serves as the potential mechanism. The results of this study provide a strong rationale for the exploration of negatively-charged aerosol as a effective therapeutic strategy for wound healing.

Acknowledgements

We would like to acknowledge Jinchang Lu (Department of Musculoskeletal Oncology, the First Affiliated Hospital of Sun Yat-sen University, Guangzhou, China) for the help with animal experiment and the expert technical assistance. We would also like to acknowledge the Experimental Animal Research Laboratory of Sun Yat-sen University for providing experimental animals and the Medical Science Experimentation Center of Sun Yat-sen University for providing the experimental facilities. This study was supported by the grant from Natural Science Foundation of Guangdong Province of China (Contract grant number: 2017A-030313498) and National Natural Science Foundation of China (NSFC, Contract grant number: 81701908).

Disclosure of conflict of interest

None.

Address correspondence to: Yingbin Xu, Department of Burns, The First Affiliated Hospital of Sun Yat-sen University, NO. 58, Zhongshan 2 Road, Guangzhou, Guangdong Province, P. R. China. Tel: 86-020-87755766-8235; E-mail: 79951927@qq.com

References

[1] Saffle JR, Sullivan JJ, Tuohig GM and Larson CM. Multiple organ failure in patients with thermal injury. Crit Care Med 1993; 21: 1673-1683.

[2] Martin P. Wound healing-aiming for perfect skin regeneration. Science 1997; 276: 75-81.

[3] Stuart BO. Deposition of inhaled aerosols. Arch Intern Med 1973; 131: 60-73.

[4] O'Doherty MJ and Miller RF. Aerosols for therapy and diagnosis. Eur J Nucl Med 1993; 20: 1201-1213.

[5] Shepherd SJ, Beggs CB, Smith CF, Kerr KG, Noakes CJ and Sleigh PA. Effect of negative air ions on the potential for bacterial contamination of plastic medical equipment. BMC Infect Dis 2010; 10: 92.

[6] Kellogg EW 3rd, Yost MG, Barthakur N and Kreuger AP. Superoxide involvement in the bactericidal effects of negative air ions on Staphylococcus albus. Nature 1979; 281: 400-401.

[7] Haddrell AE, Lewis D, Church T, Vehring R, Murnane D and Reid JP. Pulmonary aerosol delivery and the importance of growth dynamics. Ther Deliv 2017; 8: 1051-1061.

[8] Wu S, Yang R and Wang G. Anti-asthmatic effect of pitavastatin through aerosol inhalation is associated with CD4+ CD25+ Foxp3+ T cells in an asthma mouse model. Sci Rep 2017; 7: 6084.

[9] Xie X, Chen L, Zhang ZQ, Shi Y and Xie J. Clinical study on the treatment of chronic wound with negatively-charged aerosol. Int J Clin Exp Med 2013; 6: 649-654.

[10] Moncada S, Palmer RM and Higgs EA. Nitric oxide: physiology, pathophysiology, and pharmacology. Pharmacol Rev 1991; 43: 109-14

[11] Xie QW, Cho HJ, Calaycay J, Mumford RA, Swiderek KM, Lee TD, Ding A, Troso T and Na-

than C. Cloning and characterization of inducible nitric oxide synthase from mouse macrophages. Science 1992; 256: 225-228.
[12] Sessa WC, Harrison JK, Barber CM, Zeng D, Durieux ME, D'Angelo DD, Lynch KR and Peach MJ. Molecular cloning and expression of a cDNA encoding endothelial cell nitric oxide synthase. J Biol Chem 1992; 267: 15274-15276.
[13] Kimura H and Esumi H. Reciprocal regulation between nitric oxide and vascular endothelial growth factor in angiogenesis. Acta Biochimica Polonica 2003; 50: 49-59.
[14] Zhao Y, Vanhoutte PM and Leung SW. Vascular nitric oxide: beyond eNOS. J Pharmacol Sci 2015; 129: 83-94.
[15] Joshi MS, Berger PJ, Kaye DM, Pearson JT, Bauer JA and Ritchie RH. Functional relevance of genetic variations of endothelial nitric oxide synthase and vascular endothelial growth factor in diabetic coronary microvessel dysfunction. Clin Exp Pharmacol Physiol 2013; 40: 253-261.
[16] Nakagawa T. Uncoupling of the VEGF-endothelial nitric oxide axis in diabetic nephropathy: an explanation for the paradoxical effects of VEGF in renal disease. Am J Physiol Renal Physiol 2007; 292: F1665-F1672.
[17] Davidson JM. Animal models for wound repair. Arch Dermatol Res 1998; 290 Suppl: S1-S11.
[18] Eberhard A, Kahlert S, Goede V, Hemmerlein B, Plate KH and Augustin HG. Heterogeneity of angiogenesis and blood vessel maturation in human tumors: implications for antiangiogenic tumor therapies. Cancer Res 2000; 60: 1388-1393.
[19] Weidner N. Tumoural vascularity as a prognostic factor in cancer patients: the evidence continues to grow. J Pathol 1998; 184: 119-122.
[20] Livak KJ and Schmittgen TD. Analysis of relative gene expression data using real-time quantitative PCR and the 2(T)(-Delta Delta C) method. Methods 2001; 25: 402-408.
[21] Yang Y, Yin D, Wang F, Hou Z and Fang Z. In situ eNOS/NO up-regulation-a simple and effective therapeutic strategy for diabetic skin ulcer. Sci Rep 2016; 6: 30326.
[22] Vajragupta O, Boonyarat C, Murakami Y, Tohda M, Musatmoto K, Olson AJ and Watanabe H. A novel neuroprotective agent with antioxidant and nitric oxide synthase inhibitory action. Free Radic Res 2006; 40: 685-695.
[23] Noronha SM, Noronha SA, Klepp AG, Ipolito MZ, Ferreira LM and Gragnani A. Keratinocyte growth factor, interleukins (1 beta, 6, 8, 10, 12), and tumor necrosis factor alpha in culture medium of dermal fibroblast of burned patients. Acta Cir Bras 2014; 29 Suppl 1: 62-68.
[24] Zhao Y, Vanhoutte PM and Leung SW. Vascular nitric oxide: beyond eNOS. J Pharmacol Sci 2015; 129: 83-94.
[25] Jaśkowski J and Myśliwski A. Effect of air ions on healing of wounds of rat skin. Exp Pathol 1986; 29: 113-117.
[26] Chernet B and Levin M. Endogenous voltage potentials and the microenvironment: bioelectric signals that reveal, induce and normalize cancer. J Clin Exp Oncol 2013; Suppl 1.
[27] Fan L, Song J, Hildebrand PD and Forney CF. Interaction of ozone and negative air ions to control micro-organisms. J Appl Microbiol 2002; 93: 144-148.
[28] Hudlicka O and Brown MD. Adaptation of skeletal muscle microvasculature to increased or decreased blood flow: role of shear stress, nitric oxide and vascular endothelial growth factor. J Vasc Res 2009; 46: 504-512.
[29] Han X, Deng Y, Yu J, Sun Y, Ren G, Cai J, Zhu J and Jiang G. Acarbose accelerates wound healing via akt/eNOS signaling in db/db mice. Oxid Med Cell Longev 2017; 2017: 7809581.
[30] Al-Roujayee AS. Naringenin improves the healing process of thermally-induced skin damage in rats. J Int Med Res 2017; 45: 570-582.
[31] Zhang XN, Ma ZJ, Wang Y, Sun B, Guo X, Pan CQ and Chen LM. Angelica Dahurica ethanolic extract improves impaired wound healing by activating angiogenesis in diabetes. PLoS One 2017; 12: e0177862.